Available online at www.sciencedirect.com

SCIENCE DIRECT®

Surface Science 565 (2004) 89–102

www.elsevier.com/locate/susc

Theoretical study of hydrogen adsorption on the GaN(0 0 0 1) surface

V.M. Bermudez *

Naval Research Laboratory, 4555 Overlook Avenue, S.W., Washington, DC 20375-5347, USA

Received 11 March 2004; accepted for publication 22 June 2004
Available online 21 July 2004

Abstract

Ab initio density functional theory, using the B3LYP hybrid functional with all-electron basis sets, has been applied to the adsorption of H on the (0 0 0 1) surface of wurtzite GaN. For bulk GaN, good agreement is obtained with photoemission and X-ray emission data for the valence band and for the Ga 3d and N 2s shallow core levels. A band gap of $E_g = 4.14$ eV is computed vs the experimental value (at 0 K) of 3.50 eV. A simple model, consisting of a (2×2) structure with 3/4-monolayer (ML) of adsorbed H, is found to yield a density of states in poor agreement with photoemission data for H adsorbed on surfaces prepared by ion bombardment and annealing. A new model, consisting of co-adsorbed Ga (1/4 ML) and H (1/2 ML), is proposed to account for these data.
© 2004 Elsevier B.V. All rights reserved.

Keywords: Models of surface chemical reactions; Chemisorption; Gallium nitride; Hydrogen atom

1. Introduction

The chemisorption of H on GaN surfaces is a key aspect of this technologically important material. The stability of GaN at high temperature is strongly affected by the presence of H_2 in the ambient [1] which, in turn, influences the quality of material grown by metalorganic chemical vapor deposition (MOCVD). Also, H remaining from MOCVD growth and trapped in the bulk, as well as at grain boundaries and interfaces, affects the performance of GaN-based electronic devices [2].

Adsorbed H is also of fundamental interest for several reasons. The ideal Ga-polar (0 0 0 1) and N-polar $(0 0 0 \bar{1})$ surfaces are terminated in a lattice plane of Ga or N, respectively. On such surfaces, Ga (N) atoms have an electron population of 3/4 |e| (5/4 |e|) localized in dangling orbitals which would make these surfaces metallic. On either surface, adsorption of $\Theta_H = 0.75$ monolayers (ML's) of H in a (2×2) surface unit cell (where $\Theta_H = 1$ means one H per surface site) satisfies the

* Tel.: +1 202 767 6728; fax: +1 202 767 1165.
E-mail address: bermudez@estd.nrl.navy.mil

0039-6028/$ - see front matter © 2004 Elsevier B.V. All rights reserved.
doi:10.1016/j.susc.2004.06.209

"electron-counting rule" [3]. This rule requires, for a stable surface, that all bonding orbitals and N dangling orbitals be doubly-occupied and that all Ga dangling orbitals be empty. On the Ga-polar face for example, the three unpaired Ga electrons per (2×2) unit cell combine with the three electrons on the H atoms to form three Ga–H bonding orbitals. This structure, henceforth termed "(2×2)H", leaves the dangling orbital on the fourth surface Ga atom empty and renders the surface semiconducting as observed experimentally (see below). Other stabilization mechanisms (e.g., vacancies or adsorbed Ga or N) are also possible as discussed in recent reviews [4,5]. Several theoretical studies [3–11] of H adsorption on polar GaN surfaces have been performed, and most conclude that the (2×2)H structure is the most stable configuration except under growth conditions [3,11] involving a high pressure of H_2. However, to our knowledge the simple (2×2)H structure has not yet been observed experimentally. A conceptual difficulty with the observation of this structure lies in how one would stabilize the bare surface, in the experimentally-observed semiconducting state, before adsorption (or after desorption) of H.

A significant body of experimental data exists for the adsorption of H on GaN surfaces; although, a complete model has not yet been presented. Several groups have studied the vibrational spectrum [12–17], using high-resolution electron energy loss spectroscopy (HREELS), or the temperature-programmed desorption (TPD) [18–21] of adsorbed H. Others have reported electron energy loss (ELS) [22] or ultraviolet photoemission spectroscopy (UPS) [23–26] data showing H-induced structure, which is difficult to interpret without reference to a theoretical model. The HREELS and TPD studies find no surface H prior to chemisorption; although, effusion of H from the bulk of MOCVD material can be detected [18] at high temperature. Furthermore, UPS data show that adsorption of H on the clean surface removes surface states, which indicates that such surfaces are not already saturated with adsorbed H. On the other hand, ion scattering spectroscopy (ISS) studies [27,28] of the N-polar surface detect about 0.75 ML of H, even on surfaces not intentionally exposed to H atoms. The surface H is thought to arise by out-diffusion, during high-temperature annealing, of bulk H retained from MOCVD growth. It has been shown [29] that the release of H from the bulk of Mg-doped (p-type) GaN is rate-limited by the recombinative desorption of H_2 at the surface, rather than by bulk diffusion of H atoms, and that the surface coverage is low under desorption conditions.

It has been found [30–32] that, for low-energy (100 eV) electrons, the cross-section for electron-stimulated desorption (ESD) of H from the Ga-polar GaN(0001) surface is several orders of magnitude larger than for a Si(100) or (111) substrate. The charge and kinetic energy of the desorbing H and the dependence of the desorption rate on incident electron energy, all of which are important in defining the ESD mechanism [33], are unknown at present, and no corresponding data have been reported for the N-polar surface. It was also found [31] that the reduction in the ESD cross-section upon substituting D for H is only a factor of ~3 for H/GaN(0001) vs ~50 for H/Si(100). This implies that, in the former case, desorption occurs via a very long-lived excited state and/or that the kinetic energy of the desorbing particle is so high that even the more massive D atom has sufficient velocity to escape before relaxation occurs. This issue is of practical significance because of the possibility of using ESD of H for patterned etching of GaN [34].

In the present work we will attempt to understand the changes in the electronic structure of the Ga-polar GaN(0001) surface in response to a saturation coverage of adsorbed H. An essential first step is to define a model for the H-covered surface that is consistent with the available data. Furthermore, understanding the structure formed by adsorption of H can provide insight into that of the clean surfaces. The focus here will be on surfaces cleaned by ion bombardment and annealing (IBA) following exposure to ambient atmosphere, for which the majority of the available spectroscopic data (UPS, ELS, ISS, etc.) have been obtained. On the other hand, most structural studies, using low-energy electron diffraction (LEED) or scanning tunneling microscopy (STM), have been carried out on samples grown by molecular beam epitaxy (MBE) and maintained in situ. No additional sur-

face cleaning, and thus no ion bombardment or high-temperature annealing in ultra-high vacuum (UHV), is needed in this case. The surface structures resulting from the two preparation methods are different, as will be discussed below. Most of the theoretical work [1] on polar surfaces to date [3–11,35–44] has addressed primarily the surface energy under MBE or MOCVD growth conditions and/or the stability of the various structures observed in LEED or STM for samples prepared in situ by MBE. Exceptions are the works of Wang et al. [35,36] and of Strasser et al. [37] which interpret angle-resolved UPS data.

2. Computational details

Density functional theory (DFT) calculations were performed using the CRYSTAL98 suite of programs [46,47] and the B3LYP hybrid functional. This approach has been shown to give reasonably accurate band gaps for a wide range of materials [48,49] and to yield reliable structural results [50,51] for the bulk and for the clean and adsorbate-covered polar surfaces of wurtzite ZnO, which is isostructural and isoelectronic with GaN. Optimization of basis sets, bulk-lattice constants and adsorbate geometries (see below) was done using the LoptCG script [2] which computes gradients numerically by repeated runs of CRYSTAL98 and then executes a conjugate gradient procedure to locate the energy minimum.

The all-electron contracted Gaussian basis sets [2] for Ga and N were derived from those used in previous [52,53] studies of GaN. The Ga basis set consists of 6s + 5p + 2d shells (an 864111/64111/41 set), and the exponents of the outermost 3sp and 1d shells were reoptimized (using the B3LYP functional) with Ga in the bulk GaN lattice. The results were 1.8596, 0.7105 and 0.2763 for the 3sp shells and 0.6393 for the d shell. The original N basis set consists of 4s + 3p shells. A single d shell was added (a 7311/311/1 set), and the exponents of the outermost 2sp and d shells were optimized. The values found were 0.4339 and 0.1319 for the 2sp shells and 0.5972 for the d shell. The standard Pople 6-31G** basis set [3] was used for H, which consists of inner and outer s-shells of three and one Gaussian, respectively, and a single p-shell for polarization. The use of DFT in CRYSTAL98 requires auxiliary Gaussian-type basis sets for fitting the exchange-correlation potential [54]. For Ga and N, these were provided by R. Pandey (personal communication). [4] For H, the standard set of 12 s-functions, with exponents from 0.1 to 2000, was used.

Geometry optimization for the periodic slab-model surfaces with adsorbates (see below) is computationally intensive. In order to make the problem tractable we have adopted the practice, commonly used in molecular systems, of optimizing the structure at a low level and then determining the properties via a single-point calculation at a high level. In the present case, optimization of the slab-model surfaces was done at the restricted Hartree Fock (RHF) level using Durand–Barthelat effective-core pseudopotentials (ECP's) as described by Causà et al. [55] for bulk III–V semiconductors. These are large-core ECP's that treat the Ga 3d level as part of the core. The 21G* basis sets for Ga and N were derived from those given [55] for GaP and BN, respectively, with the exponents of the outer sp and d shells reoptimized

[1] It should be noted that in some theoretical work the label (0001), and not $(000\bar{1})$, is applied to the N-polar face, and comparisons are made to experimental data for which the surface polarity was not actually determined. Caution is required on the part of the reader to avoid confusion.

[2] The LoptCG script and the all-electron Gaussian basis sets were obtained at http://www.crystal.unito.it/.

[3] The H-atom basis set was obtained from the Extensible Computational Chemistry Environment Basis Set Database, Version 11/29/01, as developed and distributed by the Molecular Science Computing Facility, Environmental and Molecular Sciences Laboratory which is part of the Pacific Northwest Laboratory, P.O. Box 999, Richland, Washington 99352, USA. Contact David Feller or Karen Schuchardt for further information. The URL is http://www.emsl.pnl.gov:2080/forms/basisform.html.

[4] For Ga: 14 s-type functions with exponents from 0.1 to 6000, 2 d-type with exponents of 0.3 and 0.9 and 1 g-type with an exponent of 0.3. For N: 14 s-type functions with exponents from 0.07 to 2000, 6 p-type with exponents from 0.4 to 1.2, 4 d-type with exponents from 0.1 to 1.0, and 1 f-type and 1 g-type with exponents of 0.3 and 0.6, respectively.

for GaN. The values used were Ga: 0.191 (sp), 0.296 (d) and N: 0.255 (sp), 0.800 (d). As a test, the bulk-lattice constants obtained at the RHF/ECP level will be compared with those obtained at the B3LYP level using the all-electron basis sets described above. In calculating energies for the various possible adsorbate structures, the RHF/ECP energies were corrected for electron correlation a postiori [55] using the HF electron density and the Perdew–Wang generalized gradient approximation (PW-GGA) density functional.

Because the wurtzite (0001) and (000$\bar{1}$) surfaces are polar, special procedures were needed to assure self-consistent field (SCF) convergence [56] in the slab-model calculations. For each surface structure (see below) the RHF/ECP geometry optimization began with an SCF calculation using a high degree of Fock mixing (95%) [46]. The resulting Fock matrix was then used as the starting point for another SCF calculation with no Fock mixing, and the converged output from this second SCF was then used to initiate the geometry optimization. In the DFT slab-model calculations it was not possible to achieve SCF convergence with a Fock mixing of less than 95%.

3. Results and discussion

3.1. Bulk properties

Since this is, to our knowledge, the first DFT treatment of GaN using a hybrid functional, a brief discussion of the results for the bulk will be given.

The wurtzite lattice belongs to space group 186 ($P6_3mc$), characterized by lattice constants a and c and by $u = b/c$ where b is the Ga–N bilayer thickness. The bulk electronic structure was treated by first optimizing a, c and u at the B3LYP level with all-electron basis sets, and the resulting parameters are compared with experiment [57–59] in Table 1. These values, rather than the experimental quantities, were used in all subsequent calculations for reasons discussed elsewhere [60]. In dealing with surface structures, the RHF/ECP method described above will be used for geometry optimization; hence, Table 1 also gives bulk-lattice parameters obtained by this means. The RHF/ECP results are seen to be quite close to the more accurate DFT/all-electron values.

Fig. 1 compares UPS data [61], extending from the Fermi level to the Ga 3d shallow core level, with the computed density of states (DOS) for the optimized lattice. The computed band gap, obtained from the energy separation between the valence band maximum (VBM) and the conduction band minimum (CBM) in the DOS, is $E_g = 4.14$ eV vs the experimental value [57] of 3.50 eV at 0 K. As noted elsewhere [48], the B3LYP functional used here is found to overestimate somewhat the band gaps of several materials. The experimental, angle-integrated spectrum was recorded for an atomically-clean GaN(0001) surface in ultra-high vacuum under conditions of high surface sensitivity ($h\nu = 40.8$ eV) and high resolution (~0.18 eV). Hence, a band of surface states [61] is seen near

Table 1
Comparison of experimental and calculated bulk wurtzite GaN lattice constants

Method	a (Å)	c (Å)	c/a	u
Expt.[a]	3.1885	5.1850	1.6262	
Expt.[b]	3.190	5.189	1.627	0.377
Semi-empir.[c]	3.1876	5.1846	1.6265	
RHF/ECP[d]	3.1937	5.1876	1.6243	0.3801
B3LYP/all-e[e]	3.1899	5.1866	1.6260	0.3761

[a] From Ref. [57] for a relaxed p-type homoepitaxial film, at room temperature, with a low free-electron concentration.
[b] From Ref. [58] for a single crystal.
[c] Estimated values for pure GaN based on a theoretical study [59] of the effects of impurities on GaN lattice constants.
[d] This work, using RHF and large-core ECP's with 21G* basis sets optimized for GaN (see text).
[e] This work, using DFT with the B3LYP functional and all-electron ("all-e") basis sets optimized for GaN (see text).

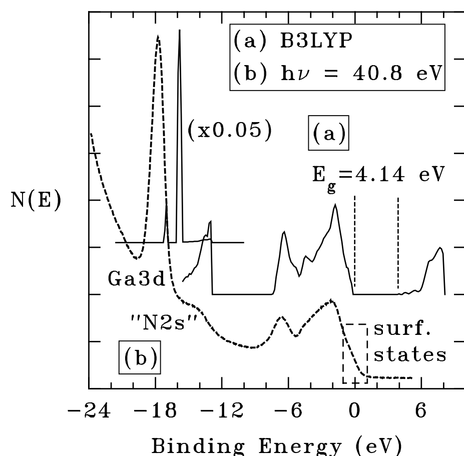

Fig. 1. Comparison of (a) the calculated DOS for bulk wurtzite GaN and (b) the experimental (surface-sensitive) UPS. Binding energy is referenced to the VBM. Structure in the DOS in the vicinity of the Ga 3d is shown on a compressed vertical scale. The "N 2s" peak, labelled as is conventional in experimental studies, is discussed in the text.

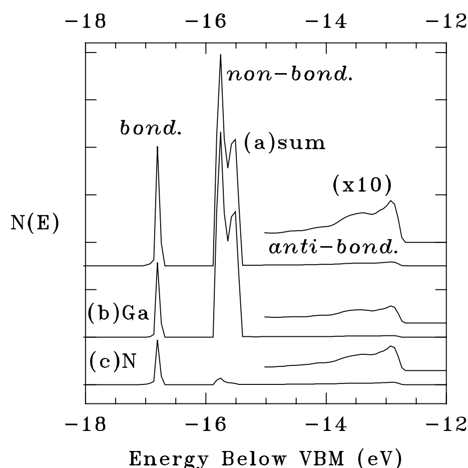

Fig. 2. Total (a) and partial (b,c) DOS's for the Ga 3d and N 2s levels. The bonding character of each band is indicated, and the anti-bonding band is repeated for each trace at 10-fold magnification.

the VBM that is absent in the bulk DOS. Neglecting the surface states, the agreement is quite good for the VB. Similarly good agreement has been found in other calculations [62–65] of the GaN DOS. The Mulliken charge on the Ga (N) atom is +(−)1.955 |e|. In the slab calculations described below, these will be taken as benchmark values for determining when a layer is sufficiently far removed from the surface to be considered "bulk-like".

The Ga 3d width and binding energy (BE) differ from experiment. The observed width is affected by the 0.45 eV spin–orbit splitting [66] (typically not resolved for GaN) and by residual disorder which can increase line width through inhomogeneous band bending. For a partially-ionic semiconductor like GaN, zero-point lattice vibration can also significantly affect experimental core-level widths [67]. None of these effects are included in the calculation.

Fig. 2 shows the Ga 3d and N 2s DOS in more detail. This part of the DOS has been extensively discussed elsewhere [63–65,68,69]. The near resonance between the Ga 3d and N 2s orbitals in the free atoms leads to covalent mixing which results in bonding and anti-bonding bands, together with non-bonding states which are nearly pure Ga 3d. The bonding character of the different bands is shown [69] in charge density plots. While the non-bonding and anti-bonding bands are easily seen in UPS (Fig. 1), the bonding band has only recently been observed [70,71], in N K-shell X-ray emission spectroscopy (XES). The dipole selection rule requires that states observed in N K-shell XES have a finite N 2p component. Orbital decomposition of the DOS (not shown) did indicate such a contribution and that it was weaker than the N 2s component.

The discrepancy between the DOS and the UPS data, as regards the Ga 3d and N 2s BE's, has been explained by Lambrecht et al. [64] in terms of the inability of DFT, with a local and energy-independent exchange-correlation potential, to model single-particle excitations of narrow bands. However, Vogel et al. [72,73] have shown that the use, within the local density approximation, of self-interaction- and relaxation-corrected pseudopotentials virtually eliminates the disagreement with experiment in the vicinity of the Ga 3d. Similar improvements in the BE's for shallow core levels were obtained for a wide range of partially-ionic semiconductors. However, the GaN VB appears to be relatively unaffected by the

corrections [73], and the band gap obtained (4.0 eV) was close to that found in the present work.

The present B3LYP results are in somewhat better agreement with experiment than are previous results which were based on fully ab initio functionals and which also neglected the self-interaction and relaxation corrections. The energy difference between the non-bonding and anti-bonding bands, about 2.7 eV, is close to the value of ~3 eV observed for the "Ga 3d" and "N 2s" peaks (Fig. 1). The computed non-bonding band lies at 15.6 eV below the VBM vs the experimental value [74] of 17.76 eV, and the bonding band falls at 1.1 eV below the non-bonding band, in good agreement with the experimental value [71] of 1.2 eV.

3.2. Adsorption of H

3.2.1. The (2 × 2)H surfaces

The first goal is to determine a structure for the H-adsorbed surfaces that will adequately model the data described above. Many theoretical studies (e.g., Refs. [3–11,35–43]) have shown that the polar GaN(0001) and (000$\bar{1}$) surfaces, when completely clean and free of defects, are energetically unfavorable in comparison to surfaces with either vacancies or adsorbates. As noted above, either autocompensation via vacancy formation or the presence of adsorbates is needed to satisfy the electron-counting rule. Since the main focus is on H-adsorption, the bare ideally-terminated surfaces are not analyzed here.

We begin with a brief examination of the well-known [3,6–11] (2 × 2)H surfaces, described above, to see if they are useful for the present purposes. Fig. 3a shows the model for the (0001)- and (000$\bar{1}$)-(2 × 2)H surfaces based on a two-dimensionally-periodic slab comprised of five Ga–N bilayers. Since the present basis sets use localized atomic orbitals, rather than plane waves, periodicity along the surface normal is not needed, and an isolated slab can be used [50,51]. Previous calculations have used slabs of four [3,6,9,35], five [8] or eight [39,41] bilayers, and it will be shown below that a five-bilayer slab is sufficiently thick to isolate the two surfaces from each other. The Ga–H and N–H distances were set at 1.58 and 1.07 Å, respectively, based on the sums of covalent radii of the respective atoms. A Ga–H distance of 1.59 Å was previously found [8] for the optimized (0001)-(2 × 2)H structure. In the present work the central (i.e., third) bilayer was essentially bulk-like in that the atom charges were ±1.958 |e|, virtually identical to the bulk value, noted above, of 1.955 |e|. In contrast, surface Ga (N) atoms bonded to H had charges of +1.80 (−1.60) |e|. The H-atom charges were −0.439 |e| for Ga–H and +0.322 |e| for N–H.

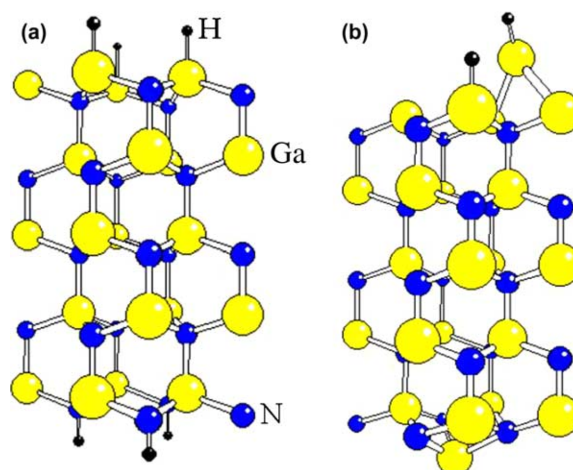

Fig. 3. (a) Slab model for the (0001)- and (000$\bar{1}$)-(2 × 2)H surfaces with $\Theta_H = 0.75$ ML. The slab consists of 5 Ga–N bilayers with three of the four atoms on either surface bonded to H. (b) One of several possible models for co-adsorbed Ga and H on the Ga-polar face with the Ga adatom in the T_4 site. The N-polar face is shown H-free with a Ga adatom in the H_3 site.

The DOS results (see below) for the (2 × 2)H slab are in qualitative agreement with those described by Fritsch et al. [8] and may be summarized as follows. [5] The Ga–H bonding orbitals on the Ga-polar face are located in a narrow region (~0.5 eV wide) near the VBM. On the N-polar face, the N doubly-occupied non-bonding lone-pair orbital produces a narrow level in the gap, just above the VBM, and the N–H bonding orbitals

[5] The band-structure results illustrated in Ref. [8] are for AlN, but the GaN results are similar and are described in the text.

occur near the bottom of the VB over a range of ∼2.5 eV. In the present case, geometry optimization was not done, but the results concur with those of Fritsch et al. [8] for which such optimization was performed. Adsorbate features are very weak in the partial DOS (PDOS) for the central GaN bilayer. Together with the bulk-like charge densities on the central bilayer (noted above), this supports the conclusion that a five-bilayer slab is sufficiently thick to isolate the two surfaces from each other.

The VB DOS's obtained for the simple (0001)-(2 × 2)H and (000$\bar{1}$)-(2 × 2)H surfaces bear little resemblance to UPS data reported to date (see below). The H-induced features seen in UPS on the Ga-polar face [23] are broad and spread essentially across the whole VB. On the N-polar face [26], there is no evidence for either N–H bonding states near the VB minimum or an N non-bonding lone-pair orbital above the VBM. The latter state occurs at ∼1.4 eV below the VBM on the clean surface [26,35] and is *removed* by H adsorption. One is then led to conclude that such (2 × 2)H structures do not adequately represent the experimental surfaces, which have been prepared by IBA followed by exposure to H atoms.

Another model for H adsorption was considered; namely, one involving a Ga–H–Ga bridge in which a three-center, two-electron (3C2E) bond is formed. Such structures are familiar in the chemistry of boranes (B_xH_y), and an In–H–In 3C2E bridge has been observed [45] in the chemisorption of H on the In-polar InP(001) surface. In that case, an In atom on an ideally-terminated surface has two dangling orbitals, each with an effective occupancy of 3/4 |e|. Electron counting can then be satisfied by forming a doubly-occupied In–In dimer bond with an In–H–In 3C2E bridge between dimers. However, an analogous structure, with electron-counting requirements fully satisfied, cannot easily form on the GaN surfaces studied here.

Yet another model could be formulated by adding only one H atom to the (2 × 2) unit cell, giving $\Theta_H = 0.25$ ML. Of the resulting four "surface" electrons (i.e., three from the surface Ga atoms and one from the H), two would form the Ga–H bond and two would form a doubly-occupied non-bonding lone-pair orbital on one of the other Ga sites. However, this structure violates the electron-counting rule described above and has not been further investigated here.

3.2.2. Models for co-adsorbed Ga and H

If adsorbed H is not directly and solely responsible for stabilizing the polar surfaces, under the conditions of interest here, then other mechanisms must be considered. Based on previous theoretical work [3–11,35–43], Ga or N adatoms or vacancies are potential candidates. The field can be narrowed by recalling that HREELS data [12,13] after exposure of the Ga-polar surface to H atoms show only Ga–H vibrations. This argues against a significant concentration of Ga vacancies or N adatoms on this surface, which would be expected to lead to the appearance of N–H modes. The temperature at which air-exposed GaN samples are typically annealed in UHV, as part of the IBA cleaning process, is in the 800–900 °C range. This is above the temperature (780 °C [75]) for congruent decomposition of GaN and corresponds to a more rapid loss of N than of Ga. Hence, a reasonable surface model in the present case may involve Ga adatoms remaining from incomplete thermal desorption of the outermost Ga–N bilayer.

Indirect evidence for the possible importance of Ga adatoms in H adsorption comes from HREELS data [15–17] for H adsorbed on GaN(000$\bar{1}$) which show (unlike the case for the Ga-polar face [12,13]) both Ga–H and N–H stretching modes. Unfortunately, the HREELS resolution (typically ∼5–10 meV) is not sufficiently high that multiple, distinct Ga–H sites can be easily distinguished on the Ga-polar surface. Further evidence comes from the observation [26] in UPS of a Ga-derived surface state on (000$\bar{1}$) surfaces prepared by IBA. The state is removed by chemisorption of H.

The adsorption of Ga on the Ga- and N-polar faces has been studied theoretically [3–11,35–43], mainly for conditions pertaining to MBE growth. For the (0001) face under Ga-rich conditions, adsorption of $\Theta_{Ga} = 0.25$ ML in a (2 × 2) structure leads to a stable surface (henceforth termed "(2 × 2)Ga") with the adatom in a T_4 site (directly above an underlayer N atom). This structure is

slightly lower in energy than one with the adatom in an H_3 site (directly above a 3-fold hollow in the N underlayer). The T_4–H_3 energy difference is predicted to be small in comparison to ΔH_{ads}, the heat of adsorption of H (see below). The three Ga–Ga backbonding orbitals are all doubly-occupied, and the dangling orbitals on the fourth lattice Ga and on the Ga adatom are empty, which satisfies electron-counting requirements.

A (0001)-(2 × 2)Ga structure has been reported in STM studies [44,76,77] following in situ MBE growth. It has, however, been suggested [76,78] that this results from a small amount of co-adsorbed As impurity, due to previous use of the MBE chamber to grow As compounds. In any case, a well-developed (2 × 2) LEED pattern is not generally seen for surfaces prepared by IBA (Refs. [29,79] and works cited). Instead a (1 × 1) pattern is found (often accompanied by faceting) which suggests a poorly-ordered surface, possibly with a random array of Ga adatoms. This is different from the pseudo-(1 × 1) adlayer structure, involving two full monolayers of adsorbed Ga, which is seen under Ga-rich MBE conditions [38,39]. For the IBA (1 × 1) surface, UPS data show no evidence of metallic character in the form of emission at the Fermi level, and a high coverage of Ga–Ga bonds is not detected in surface-sensitive Ga 3d XPS (e.g., Ref. [61]). For a monolayer of Ga on the GaN surface [80], the adlayer Ga 3d appears as a distinct shoulder at ~1.4 eV lower BE than that of bulk GaN, and a Ga bilayer results in an even larger chemical shift. It has been shown [81,82] that a (2 × 2) surface (which indicates a Ga-polar face [83]) can be obtained when air-exposed samples are cleaned by annealing in NH_3 vapor [6] (without ion bombardment); however, another study [84] found only a (1 × 1) surface for a similar treatment.

[6] A (0001)-(2 × 2)N structure, involving N adatoms, is known to be intrinsic to the Ga-polar face grown under N-rich MBE conditions (Ref. [78] and works cited). It is possible that this, rather than Ga adatoms, might be the origin of the (2 × 2) structures reported in Refs. [81,82]. However, for reasons given above, it is considered unlikely that a significant coverage of N adatoms occurs on the IBA-cleaned Ga-polar surface.

In the following, we will invoke a (2 × 2)Ga structure as a model for the local environment of a Ga adatom and use this as a starting point for the subsequent adsorption of H. This is based on the theoretical stability of this structure and on the experimental evidence, noted above, for the importance of Ga adatoms. We put aside the question of whether a pure (2 × 2)Ga phase exists, under typical conditions, as a stable, macroscopic entity on the Ga-polar surface. The Ga adatom is initially placed in a T_4 site; however, due to the small T_4–H_3 energy difference (see below), it is necessary to consider the possibility that H adsorption causes a displacement of the adatom to the H_3 site. It is noted in this regard that the activation barrier for hopping between T_4 and H_3 is calculated [85] to be 0.4 eV.

Adsorption of two H atoms on a (2 × 2)Ga surface leads to structures like that shown in Fig. 3b, which continue to satisfy the electron-counting rule. One of the three Ga–Ga adatom backbonds is broken, and there are then six possible structures as shown in Fig. 4. Whichever Ga is vacant (i.e., not bonded to H or to the Ga adatom) then exhibits an unoccupied dangling orbital. Including the possibility of $T_4 \rightarrow H_3$ displacement then leads to a total of 12 inequivalent structures. In the following, structures will be labelled "Ga(T_4) + 2H(a)", etc. to specify the Ga and H sites with reference to Fig. 4. Finally, in defining the structures in Fig. 4, no distinction has been made between inequivalent Ga sites 2 and 4 (see Fig. 4a). Additional unique structures could be formed by moving the adsorbed H from site 4 to site 2 in models (a) and (c). Since these sites are related by an *approximate, local* mirror plane (not a true mirror plane) we expect these to be energetically equivalent, which will be justified below.

The first step was to obtain the geometries and energies of the H-free (2 × 2)Ga(T_4) and Ga(H_3) structures. These results are needed in estimating ΔH_{ads}, and they also serve as a check of the calculational procedure. In either case, the adatom position was optimized while keeping the rest of the slab fixed. The height of the Ga(T_4) adatom above the terminating Ga plane was found to be 1.66 Å vs previously-reported values of 1.78 Å [8], 1.66 Å [38] and 1.73 Å [44]. For Ga(H_3) the height

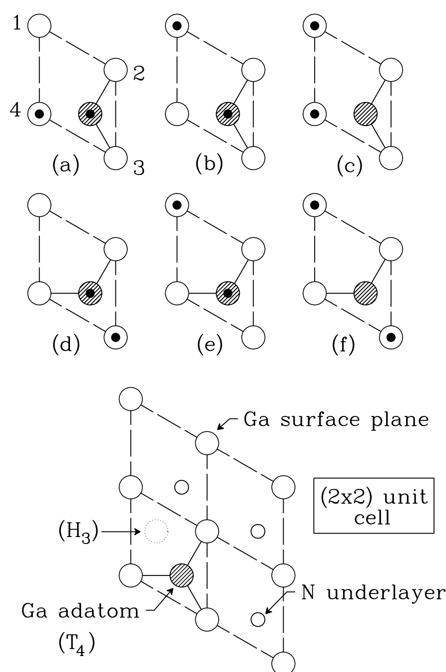

Fig. 4. Schematic diagram showing six possible structures, derived from the (2×2)Ga surface, after adsorption of two H atoms per unit cell. The solid circles are H atoms, and the solid lines show backbonds from the Ga adatom to the surface. In (a), the inequivalent Ga sites are numbered for reference in the text. The adatom is shown in the T_4 site, and another six structures could be drawn with the H_3 site occupied. These are model structures only and have not been optimized. Also shown is a diagram for the H-free (2×2)Ga unit cell with the Ga adatom in the T_4 site and with the empty H_3 site indicated.

above the surface plane was 1.72 Å vs a previous value [38] of 1.63 Å. The H_3 site was found to be higher in energy than the T_4 by 0.69 eV per (2×2) unit cell based on the RHF/ECP energies after correction for electron correlation as described above. This compares with previous results of 0.6 eV [8] and 0.12 eV [38]. A vanishingly-small energy difference was found in Ref. [85]. In these and in subsequent calculations the N-polar face was "passivated" with one Ga adatom per (2×2) unit cell in the H_3 site which has been found (e.g., Ref. [8]) to be the most stable structure for this face at low Ga coverage.

Previous studies of the (0001)-(2×2)Ga(T_4) structure found that the only relaxation of the substrate is a small outward displacement of the outermost Ga layer by 0.13 Å [8] or 0.10 Å [44], relative to the ideally-terminated position. An even smaller relaxation, 0.05 Å, is found [8] for the (2×2)H surface described above. Hence, in the present study, only the Ga and H adatom positions were adjusted in the geometry optimizations.

Table 2
Computed heats of adsorption, per (2×2) unit cell, for the (2×2)Ga + 2H co-adsorbed structures shown in Fig. 4

Structure[a]	ΔH_{ads} (eV)
Ga(T_4) + 2H(a)	6.33
Ga(T_4) + 2H(b)	6.35
Ga(T_4) + 2H(c)	8.30
Ga(T_4) + 2H(d)	6.32
Ga(T_4) + 2H(e)	6.24
Ga(T_4) + 2H(f)	8.43
Ga(H_3) + 2H(a)	6.49
Ga(H_3) + 2H(c)[b]	8.05
Ga(H_3) + 2H(f)	8.03

[a] The labelling of the structures is described in the text and in Fig. 4.
[b] For this structure (referring to Fig. 4c) the H atom on site 1 is moved to site 3, and the Ga adatom backbonds are to sites 1 and 2.

All six of the Ga(T_4) + 2H structures indicated in Fig. 4 were subjected to geometry optimization at the RHF/ECP level. The coordinates of each of the three adsorbed atoms (one Ga plus two H) were optimized while atoms in the slab itself were frozen in the ideal, bulk-lattice positions. For each structure, ΔH_{ads} (Table 2) was obtained using

$$E[(2\times2)\mathrm{Ga}(T_4)] + 2 * E[\mathrm{H}] = E[\mathrm{Ga}+2\mathrm{H}] + 2 * E_{ZP}(\mathrm{Ga{-}H}) + \Delta H_{ads}$$

where $E[(2\times2)\mathrm{Ga}(T_4)]$ and $E[\mathrm{Ga}+2\mathrm{H}]$ are, respectively, the total RHF/ECP energies of the (2×2)Ga surface before and after H co-adsorption. Both values were corrected a postiori for electron correlation as described above. E_{ZP}(Ga–H) is the zero-point vibrational energy of an adsorbed H atom, and E[H] is the energy of a free H atom. Based on HREELS data [12,13], E_{ZP}(Ga–H) = 0.116 eV. Any H-induced change in the vibrational modes of the slab is neglected in estimating the total E_{ZP}. A value of E[H] = −13.558 eV was found for the present H-atom basis set which is close to the experimental value of −13.606 eV. The ΔH_{ads} computation uses two H

atoms, rather than an H_2 molecule, since the adsorption experiments involve dissociation of H_2 by a hot (~2000 K) tungsten filament. Molecular H_2 is not known to chemisorb readily on the GaN(0001) surface at room temperature under UHV conditions.

The results in Table 2 indicate that Ga(T_4) + 2H(f) is the most energetically-favorable structure. The optimized interatomic distances are given in Fig. 5a. Various aspects of the results are noteworthy. Firstly, adsorption of H on the Ga adatom is unfavorable in comparison to having both H's on lattice Ga sites. Mulliken population analysis (at the RHF/ECP level) shows that the effective charge on the Ga adatom in Ga(T_4) + 2H(f) is +0.31 |e|; whereas, the charge on the Ga atoms bonded to H is +1.07 |e|. Given the H effective charge of about −0.37 |e| it is evident that the lattice Ga sites should be favored. Secondly, the virtually identical H_{ads} values for (a) and (d) and for (b) and (e) indicate that, all else being equal, it makes little difference which of the three Ga–Ga backbonds is broken. This supports the approximation, noted above, of treating Ga sites 2 and 4 as being equivalent.

A third point is that the ΔH_{ads} values are quite large, e.g., 4.2 eV/Ga–H bond for Ga(T_4) + 2H(f) vs 4.5 eV for the bond energy in H_2 [86]. Strain in the Ga–Ga backbonds for the H-free (2 × 2)Ga surface probably makes a significant contribution to ΔH_{ads}. In structures with one H on the adatom the local geometry of the Ga adatom is seen to be nearly planar (Fig. 5b) as expected for 3-fold coordinated Ga in a free molecule [86]. When one of the three backbonds is broken, the adatom is free to relax away from the ideal T_4 position and into this nearly-planar configuration.

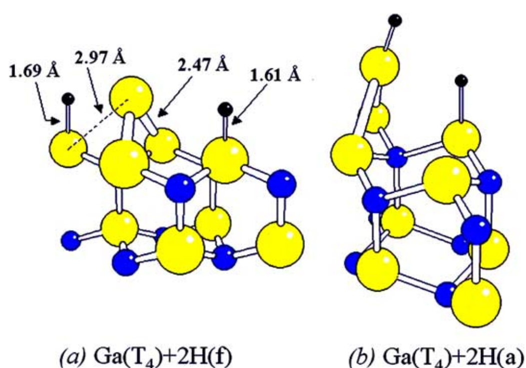

Fig. 5. (a) Schematic diagram showing the optimized surface structure for the lowest-energy model (see Table 2), Ga(T_4) + 2H(f). For clarity, only the uppermost two Ga–N bilayers are shown. (b) Similar to (a) but for a structure with one H on the Ga adatom, Ga(T_4) + 2H(a). The adatom Ga–H bond makes an angle of 7.8° with the adatom Ga–Ga–Ga plane.

The ΔH_{ads} obtained here is not in good agreement with the experimental value [29] of, at most, 2.44 eV/Ga–H bond which is based on the kinetics of hydrogen release at 700–900 °C. However, the configuration of the H-covered surface under such conditions may differ from that in the 0 K limit appropriate to the present calculations. For example, if desorption at $\geqslant$ 700 °C occurs not from the Ga(T_4) + 2H(f) configuration but from the Ga(T_4) + 2H(a) as an intermediate state, then a ΔH_{ads} of about 3.12 eV/Ga–H bond would be expected (cf. Table 2), in somewhat better agreement with experiment. Including the thermal excitation of the Ga–H vibrational mode at $\geqslant$ 700 °C would further reduce the theoretical estimate of the desorption energy.

A final point is that the presence of adsorbed H appears to reduce the T_4–H_3 energy difference. As noted above, the present RHF/ECP result places the H-free Ga(H_3) site 0.69 eV higher than the Ga(T_4); whereas, for example, the Ga(H_3) + 2H(f) structure lies only 0.40 eV higher than the Ga(T_4) + 2H(f). Although the effect of H on the activation barrier for $T_4 \leftrightarrow H_3$ hopping is unknown, the results suggest that co-adsorption of H during MOCVD might possibly promote two-dimensional growth by enhancing Ga adatom surface diffusion.

We have also obtained the energy difference, ΔE, between the Ga(T_4) + 2H(f) structure and the (2 × 2)H surface, described above, after optimizing the positions of the three H atoms in the latter unit cell. An optimized Ga–H distance of 1.60 Å was obtained. The energy difference is given by

$$\Delta E = E[\mathrm{Ga}(\mathrm{T}_4) + 2\mathrm{H}(\mathrm{f})] - E[(2 \times 2)\mathrm{H}] - E(\mathrm{Ga}) + E(\mathrm{H})$$

where $E(\text{Ga})$ and $E(\text{H})$ are the energies of the respective free atoms obtained for the basis sets used in the slab calculations. The result is $\Delta E = -2.5$ eV, i.e., the Ga(T_4) + 2H(f) is the more stable structure.

3.2.3. Electronic structure of co-adsorbed Ga and H

Having determined the most energetically-favorable structure we will now examine its electronic properties using DFT with the B3LYP functional and the all-electron basis sets described above. Figs. 6 and 7 show the valence band UPS difference spectrum, $\Delta N(E)$, for adsorbed H in comparison with the computed PDOS derived from adsorbed H (Fig. 6) and from surface and adatom Ga's (Fig. 7). The $\Delta N(E)$ data were obtained [30] by subtracting the clean-surface spectrum from that recorded after H adsorption. The clean-surface spectrum was shifted (to account for a change in band-bending) and scaled so as to minimize the residual Ga 3d intensity in $\Delta N(E)$. As is typical in angle-integrated UPS studies of adsorption on GaN(0001) [23,61,87], a "negative" feature appears in $\Delta N(E)$ just above the VBM due to removal of surface states characteristic of the clean surface prepared by IBA.

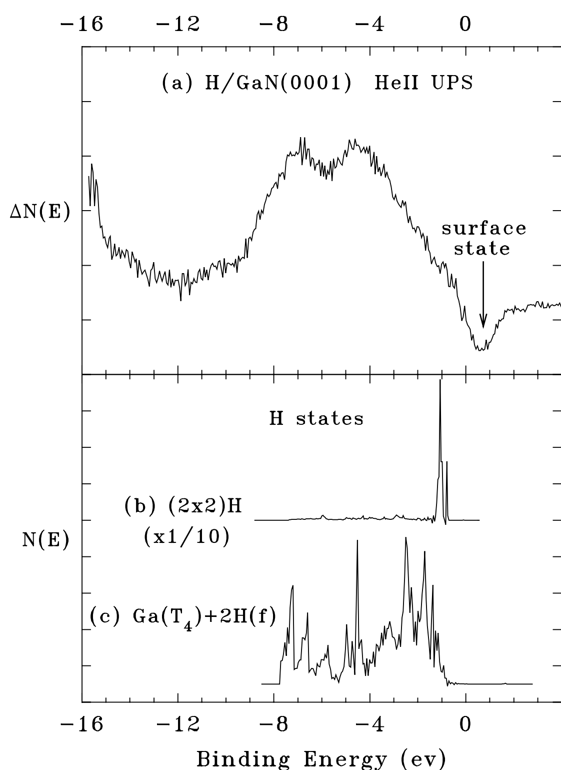

Fig. 6. Comparison of UPS data for H/GaN(0001) with calculated results. (a) HeII UPS difference spectrum (adsorbed minus clean), Ref. [30]. The resolution is about 0.8 eV. (b,c) Calculated H-derived states for the (2 × 2)H and Ga(T_4) + 2H(f) surfaces. All binding energies are referenced to the VBM. For trace (a), the VBM was found by linear extrapolation of the VB edge to zero intensity. For traces (b) and (c) the VBM was determined from the PDOS of the innermost Ga–N bilayer. The vertical scale for (b) has been reduced by a factor of 10 relative to that of (c).

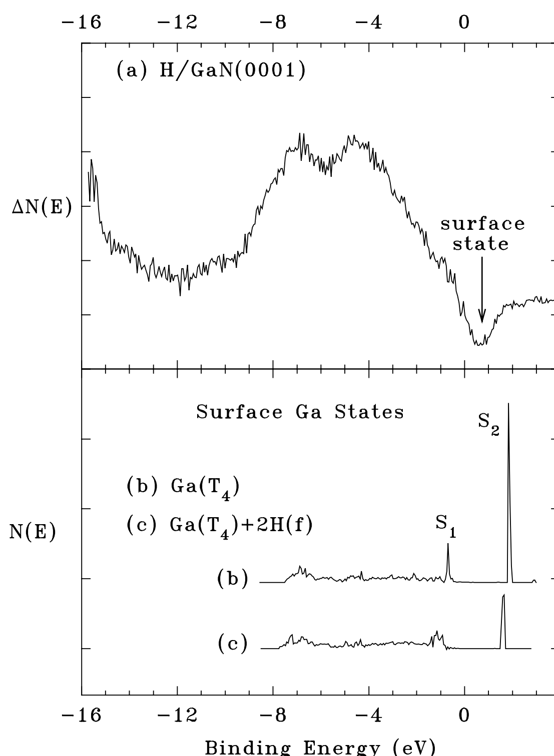

Fig. 7. Similar to Fig. 6 but showing a comparison of the data with the calculated PDOS for the four surface Ga atoms and the one Ga adatom in the (2 × 2) unit cell (cf. Fig. 4). (a) Same as in Fig. 6. (b,c) The Ga(T_4) surface before and after formation of the Ga(T_4) + 2H(f) structure. Binding energy is referenced to the VBM. S_1 and S_2 are surface states on the bare (H-free) surface that are affected by adsorption of H.

Fig. 6b shows the H PDOS for the (2 × 2)H model, described above, which concurs with previous results [6,8]. As noted above, the H-derived

states on the Ga-polar face are concentrated near the VBM, in conflict with the data which show these states to be distributed essentially throughout the whole VB. Much better agreement is found for the $Ga(T_4) + 2H(f)$ structure. It is useful to consider why the H PDOS is so different for the two structures. For the $Ga(T_4) + 2H(f)$, adsorption may be visualized as occurring in three steps; namely, breaking a Ga–Ga backbond, redistribution of charge to form two singly-occupied Ga dangling orbitals and, finally, formation of two Ga–H bonding orbitals. The intermediate step is a relaxed excited state of the initial structure, and the wavefunction of this state will be a combination of many occupied and virtual orbitals of the ground state. This is reflected in the spread of the H contribution over a wide energy range in the final adsorbed state. For the (2×2)H, on the other hand, the ground state of the (hypothetical) bare (2×2) surface unit cell already exhibits occupied Ga dangling orbitals, and no extensive mixing of occupied and virtual orbitals is needed to "prepare" the surface for adsorption.

Fig. 7b shows two Ga-derived surface states on the H-free surface. State S_1 lies below the VBM and is localized largely on the adatom. State S_2, which is derived from adatom Ga–Ga backbonds, lies in the gap at ~1.2 eV higher energy than the experimentally-observed surface state. These results are qualitatively consistent with those of Fritsch et al. [8] which is, to our knowledge, the only previous work to present surface-state bands specifically for the (0001)-$(2 \times 2)Ga(T_4)$ structure. [5] Their results show an S_1 state (comprised of adatom s-orbitals) lying slightly above the VBM and an S_2 adatom backbonding state lying somewhat farther into the gap. In the present work, adsorption of H (Fig. 7c) strongly attenuates and/or broadens S_1. The S_2 state shifts and broadens slightly in response to H and decreases in intensity when one of the three adatom backbonds is broken. However, S_2 is not completely eliminated by H adsorption which is an apparent discrepancy with experiment [25].

Comparison can also be made to the angle-resolved UPS results of Chao et al. [25]. These were obtained for a sample of unspecified polarity which, however, was grown by MOCVD on a Si-polar 6H–SiC(0001) surface and which we thus assume to be Ga-polar. Two non-dispersive, H-sensitive states were observed at or just below the VBM on the clean surface which could correspond to S_1 and S_2. A third, highly-dispersive surface state was also observed which is not found in the present calculations. On the N-polar face, a similar highly-dispersive surface state [26] has been interpreted [35] in terms of a (1×1) Ga adlayer with interacting Ga dangling orbitals. Such a structure is not included in the present model. Also, no H-induced features were observed by Chao et al. [25]; however, $\Delta N(E)$ spectra were not presented, which could mean that the very broad and nearly-structureless emission due to Ga–H orbitals was overlooked.

4. Summary and conclusions

Ab initio computational methods have been applied to the adsorption of H on the GaN(0001) surface. The results are as follows.

(1) Density functional theory with the B3LYP hybrid functional gives a good description of the bulk lattice and electronic structure of wurtzite GaN. In particular, the results for the hybridization of the Ga 3d and N 2s levels is in somewhat better agreement with experiment than are previous results using other functionals.
(2) The ideal H-stabilized (0001)-(2×2)H structure, with 0.75 ML of adsorbed H, does not account for UPS data for H on GaN(0001) surfaces cleaned by ion bombardment followed by high-temperature annealing in UHV.
(3) A new model is proposed which gives results in better agreement with UPS data. Here, 0.50 ML of H adsorbs on a (2×2)Ga structure with 0.25 ML of adsorbed Ga. Both H atoms in the (2×2) unit cell adsorb on surface-plane Ga sites, leaving the Ga adatom free of H.

The model developed here provides a reasonably good description of the UPS data for IBA sur-

faces with adsorbed H and is consistent with other results suggesting the presence of Ga adatoms on H-free surfaces prepared by IBA. Although the model provides a starting point for understanding the unusually large ESD cross-section for H/GaN(0001), it has not yet provided any direct insight into the mechanism for this effect. For example, evidence was looked for (but not found) to suggest a significantly higher degree of Ga–H vs Ga–N bond covalency. Such an effect, were it to exist, would enhance the rate for Auger decay of a Ga 3d core hole via a process involving one or both electrons in the Ga–H bond, relative to decay through an interatomic process involving the N nearest-neighbors in the partially-ionic GaN lattice.

Acknowledgments

This work was supported by the Office of Naval Research and by a grant of computer time from the DOD High-Performance Computing Modernization Program at the ASC-MSRC, Wright–Patterson AFB. A. Wander is thanked for helpful advice on overcoming SCF convergence problems, and R. Pandey is thanked for providing the Ga and N DFT auxiliary basis sets. Critical readings of the manuscript by B.I. Dunlap, C.A. Pignedoli and J. Pollmann were of great value. Xiaofeng Duan (ASC-MSRC) is gratefully acknowledged for generously providing extensive help in the use of the software.

References

[1] D.D. Koleske, A.E. Wickenden, R.L. Henry, J.C. Culbertson, M.E. Twigg, J. Cryst. Growth 223 (2001) 466.
[2] S.J. Pearton, H. Cho, F. Ren, J.-I. Chyi, J. Han, R.G. Wilson, MRS Internet J. Nitride Semicond. Res. 5S1 (2000) 10.6.
[3] C.G. Van de Walle, J. Neugebauer, J. Vac. Sci. Technol. B 20 (2002) 1640.
[4] R.M. Feenstra, J.E. Northrup, J. Neugebauer, MRS Internet J. Nitride Semicond. Res. 7 (2002) 3.
[5] J. Neugebauer, Phys. Stat. Sol. B 227 (2001) 93.
[6] K. Rapcewicz, M. Buongiorno Nardelli, J. Bernholc, Phys. Rev. B 56 (1997) R12725.
[7] J. Elsner, M. Haugk, G. Jungnickel, Th. Frauenheim, Solid State Commun. 106 (1998) 739.
[8] J. Fritsch, O.F. Sankey, K.E. Schmidt, J.B. Page, Phys. Rev. B 57 (1998) 15360.
[9] C.A. Pignedoli, R. Di Felice, C.M. Bertoni, Phys. Rev. B 64 (2001) 113301.
[10] C.A. Pignedoli, R. Di Felice, C.M. Bertoni, Surf. Sci. 547 (2003) 63.
[11] C.G. Van de Walle, J. Neugebauer, Phys. Rev. Lett. 88 (2002) 066103.
[12] V.J. Bellitto, B.D. Thoms, D.D. Koleske, A.E. Wickenden, R.L. Henry, Surf. Sci. 430 (1999) 80.
[13] V.J. Bellitto, Y. Yang, B.D. Thoms, D.D. Koleske, A.E. Wickenden, R.L. Henry, Surf. Sci. 442 (1999) L1019.
[14] S.P. Grabowski, H. Nienhaus, W. Mönch, Surf. Sci. 454–456 (2000) 498.
[15] U. Starke, S. Sloboshanin, F.S. Tautz, A. Seubert, J.A. Schaefer, Phys. Stat. Sol. A 177 (2000) 5.
[16] S. Sloboshanin, F.S. Tautz, V.M. Polyakov, U. Starke, A.S. Usikov, B.Ja. Ber, J.A. Schaefer, Surf. Sci. 427–428 (1999) 250.
[17] F.S. Tautz, S. Sloboshanin, U. Starke, J.A. Schaefer, J. Phys.: Condens. Matter 11 (1999) 8035.
[18] M.E. Bartram, J.R. Creighton, MRS Internet J. Nitride Semicond. Res. 4S1 (1999) G3.68.
[19] R. Shekhar, K.V. Jensen, Surf. Sci. 381 (1997) L581.
[20] C.-M. Chiang, S.M. Gates, A. Bensaoula, J.A. Schultz, Chem. Phys. Lett. 246 (1995) 275.
[21] Y. Yang, J. Lee, B.D. Thoms, D.D. Koleske, R.L. Henry, Mater. Res. Soc. Symp. Proc. 693 (2002) I6.48.
[22] V.J. Bellitto, B.D. Thoms, D.D. Koleske, A.E. Wickenden, R.L. Henry, Phys. Rev. B 60 (1999) 4816.
[23] V.M. Bermudez, Chem. Phys. Lett. 317 (2000) 290.
[24] S.S. Dhesi, C.B. Stagarescu, K.E. Smith, D. Doppalapudi, R. Singh, T.D. Moustakas, Phys. Rev. B 56 (1997) 10271.
[25] Y.-C. Chao, C.B. Stagarescu, J.E. Downes, P. Ryan, K.E. Smith, D. Hanser, M.D. Bremser, R.F. Davis, Phys. Rev. B 59 (1999) R15586.
[26] P. Ryan, Y.-C. Chao, J. Downes, C. McGuinness, K.E. Smith, A.V. Sampath, T.D. Moustakas, Surf. Sci. 467 (2000) L827.
[27] M.M. Sung, J. Ahn, V. Bykov, J.W. Rabalais, D.D. Koleske, A.E. Wickenden, Phys. Rev. B 54 (1996) 14652.
[28] J. Ahn, M.M. Sung, J.W. Rabalais, D.D. Koleske, A.E. Wickenden, J. Chem. Phys. 107 (1997) 9577.
[29] W.R. Wampler, S.M. Myers, J. Appl. Phys. 94 (2003) 5682.
[30] V.M. Bermudez, D.D. Koleske, A.E. Wickenden, Appl. Surf. Sci. 126 (1998) 69.
[31] V.J. Bellitto, B.D. Thoms, D.D. Koleske, A.E. Wickenden, R.L. Henry, Phys. Rev. B 60 (1999) 4821.
[32] Y. Yang, J. Lee, B.D. Thoms, Mater. Res. Soc. Symp. Proc. 743 (2003) L.11.30.
[33] R.D. Ramsier, J.T. Yates Jr., Surf. Sci. Repts. 12 (1991) 243.
[34] H.P. Gillis, M.B. Christopher, K.P. Martin, D.A. Choutov, MRS Internet J. Nitride Semicond. Res. 4S1 (1999) G8.2.

[35] F.-H. Wang, P. Krüger, J. Pollmann, Surf. Sci. 499 (2002) 193.
[36] F.-H. Wang, P. Krüger, J. Pollmann, Phys. Rev. B 64 (2001) 035305.
[37] T. Strasser, C. Solterbeck, F. Starrost, W. Schattke, Phys. Rev. B 60 (1999) 11577.
[38] A.R. Smith, R.M. Feenstra, D.W. Greve, M.-S. Shin, M. Skowronski, J. Neugebauer, J.E. Northrup, Surf. Sci. 423 (1999) 70.
[39] J.E. Northrup, J. Neugebauer, R.M. Feenstra, A.R. Smith, Phys. Rev. B 61 (2000) 9932.
[40] K. Nakamura, T. Hayashi, A. Tachibana, K. Matsumoto, J. Cryst. Growth 221 (2000) 765.
[41] A. Ishii, D. Miyake, T. Aisaka, Jpn. J. Appl. Phys. 41 (2002) L842.
[42] A. Ishii, T. Aisaka, Phys. Stat. Sol. C 0 (2003) 2490.
[43] C.G. Van de Walle, J. Neugebauer, J. Cryst. Growth 248 (2003) 8.
[44] Q.-K. Xue, Q.Z. Xue, R.Z. Bakhtizin, Y. Hasegawa, I.S.T. Tsong, T. Sakurai, T. Ohno, Phys. Rev. Lett. 82 (1999) 3074.
[45] K. Raghavachari, Q. Fu, G. Chen, L. Li, C.H. Li, D.C. Law, R.F. Hicks, J. Am. Chem. Soc. 124 (2002) 15119.
[46] V.R. Saunders, R. Dovesi, C. Roetti, M. Causà, N.M. Harrison, R. Orlando, C.M. Zicovich-Wilson, CRYSTAL98 (vers. 1.01) User's Manual, Università di Torino, Torino, 1999.
[47] C. Pisani, R. Dovesi, C. Roetti, Hartree-Fock Ab Initio Treatment of Crystalline Systems, Springer, Berlin, 1988 (Chap. 3).
[48] J. Muscat, A. Wander, N.M. Harrison, Chem. Phys. Lett. 342 (2001) 397.
[49] W.F. Perger, Chem. Phys. Lett. 368 (2003) 319.
[50] A. Wander, F. Schedin, P. Steadman, A. Norris, R. McGrath, T.S. Turner, G. Thornton, N.M. Harrison, Phys. Rev. Lett. 86 (2001) 3811.
[51] A. Wander, N.M. Harrison, J. Chem. Phys. 115 (2001) 2312.
[52] R. Pandey, J.E. Jaffe, N.M. Harrison, J. Phys. Chem. Solids 55 (1994) 1357.
[53] R. Pandey, M. Causà, N.M. Harrison, M. Seel, J. Phys.: Condens. Matter 8 (1996) 3993.
[54] M.D. Towler, A. Zupan, M. Causà, Comput. Phys. Commun. 98 (1996) 181.
[55] M. Causà, R. Dovesi, C. Roetti, Phys. Rev. B 43 (1991) 11937.
[56] A. Wander, personal communication.
[57] J.H. Edgar, S. Strite, I. Akasaki, H. Amano, C. Wetzel (Eds.), Properties, Processing and Applications of Gallium Nitride and Related Semiconductors, IEE-INSPEC, Hertfordshire, 1999.
[58] H. Schulz, K.H. Thiemann, Solid State Commun. 23 (1977) 815.
[59] C.G. Van de Walle, Phys. Rev. B 68 (2003) 165209.
[60] J.R.B. Gomes, I. de P.R. Moreira, P. Reinhardt, A. Wander, B.G. Searle, N.M. Harrison, F. Illas, Chem. Phys. Lett. 341 (2001) 412.
[61] V.M. Bermudez, J.P. Long, Surf. Sci. 450 (2000) 98.
[62] Y.-N. Xu, W.Y. Ching, Phys. Rev. B 48 (1993) 4335.
[63] V. Fiorentini, M. Methfessel, M. Scheffler, Phys. Rev. B 47 (1993) 13353.
[64] W.R.L. Lambrecht, B. Segall, S. Strite, G. Martin, A. Agarwal, H. Morkoç, A. Rockett, Phys. Rev. B 50 (1994) 14155.
[65] B. Bouhafs, F. Litimein, Z. Dridi, P. Ruterana, Phys. Stat. Sol. B 236 (2003) 61.
[66] T. Miller, T.-C. Chiang, Phys. Rev. B 29 (1984) 7034.
[67] V.M. Bermudez, J.P. Long, Appl. Phys. Lett. 66 (1995) 475.
[68] A.F. Wright, J.S. Nelson, Phys. Rev. B 50 (1994) 2159.
[69] P. Dudešek, Ľ. Benco, C. Daul, K. Schwarz, J. Phys.: Condens. Matter 10 (1998) 7155.
[70] C.B. Stagarescu, L.-C. Duda, K.E. Smith, J.H. Guo, J. Nordgren, R. Singh, T.D. Moustakas, Phys. Rev. B 54 (1996) R17335.
[71] L.-C. Duda, C.B. Stagarescu, J. Downes, K.E. Smith, D. Korakakis, T.D. Moustakas, J. Guo, J. Nordgren, Phys. Rev. B 58 (1998) 1928.
[72] D. Vogel, P. Krüger, J. Pollmann, Phys. Rev. B 54 (1996) 5495.
[73] D. Vogel, P. Krüger, J. Pollmann, Phys. Rev. B 55 (1997) 12836.
[74] J.R. Waldrop, R.W. Grant, Appl. Phys. Lett. 68 (1996) 2879.
[75] D.D. Koleske, A.E. Wickenden, R.L. Henry, W.J. DeSisto, R.J. Gorman, J. Appl. Phys. 84 (1998) 1998.
[76] V. Ramachandran, C.D. Lee, R.M. Feenstra, A.R. Smith, D.W. Greve, Phys. Rev. Lett. 84 (2000) 4014.
[77] Q.-Z. Xue, Q.K. Xue, S. Kuwano, J.T. Sadowski, K.F. Kelly, T. Sakurai, T. Ohno, Phys. Rev. Lett. 84 (2000) 4015.
[78] S. Vézian, F. Semond, J. Massies, D.W. Bullock, Z. Ding, P.M. Thibado, Surf. Sci. 541 (2003) 242.
[79] W.T. Manske, A.S. Ratkovich, C.J. Lemke, M.T. McEllistrem, J. Vac. Sci. Technol. A 21 (2003) 506.
[80] A. Barinov, L. Gregoratti, B. Kaulich, M. Kiskinova, Chem. Phys. Chem. 3 (2002) 1019.
[81] R.A. Oliver, C. Nörenberg, M.G. Martin, A. Crossley, M.R. Castell, G.A.D. Briggs, Appl. Surf. Sci. 214 (2003) 1.
[82] S.W. King, J.P. Barnak, M.D. Bremser, K.M. Tracy, C. Ronning, R.F. Davis, R.J. Nemanich, J. Appl. Phys. 84 (1998) 5248.
[83] A.R. Smith, R.M. Feenstra, D.W. Greve, M.-S. Shin, M. Skowronski, J. Neugebauer, J.E. Northrup, Appl. Phys. Lett. 72 (1998) 2114.
[84] K.M. Tracy, W.J. Mecouch, R.F. Davis, R.J. Nemanich, J. Appl. Phys. 94 (2003) 3163.
[85] T. Zywietz, J. Neugebauer, M. Scheffler, Appl. Phys. Lett. 73 (1998) 487.
[86] F.A. Cotton, G. Wilkinson, Advanced Inorganic Chemistry, fifth ed., Wiley, New York, 1988.
[87] C.I. Wu, A. Kahn, J. Appl. Phys. 86 (1999) 3209.